Redox Catalysis of Absorption from Reactive Bubbles near Electrodes

Electrolyzing sparingly soluble gases as they are absorbed from bubbles can be significantly facilitated by addition of a soluble redox couple which serves to increase both mass and charge transfer rates. A diffusion layer model is used to calculate reaction-catalyzed mass transfer rates in regions of boundary layer penetration by reactive bubbles for the case of (m, n)-order irreversible homogeneous reaction. The dissolved redox catalyst is continuously regenerated at the solid electrode surface. Approximate solutions, which relate surface flux to concentration driving force, are in excellent agreement with the numerical solutions under conditions of fast homogeneous reaction and concentrated catalyst (modified Damköhler number and dimensionless catalyst concentration greater than 3). Diffusion layer thickness is calculated from the mass transfer coefficient k_p in penetrated regions. A model based on spherical penetrating bubbles is used to determine k_p and specific surface area a_p of penetrated regions from $k_p a_p$ values that have been measured in gas-liquid flow through a packed bed. The mass transfer behavior provides useful insight into why the penetration process is so effective in increasing overall reaction rates.

Ken M. Takahashi
Richard C. Alkire
Department of Chemical Engineering
University of Illinois
Urbana, IL 61801

Introduction

In recent years there has been considerable interest in the development of new electrochemical routes for syntheses, particularly for specialty chemicals for which high yields are essential for economic reasons. Along with this industrial interest has come an increased effort to understand fundamental phenomena that control the behavior of electrodes and to develop the engineering principles necessary to design and optimize electrochemical reactors.

Reactants such as gases and nonpolar organic liquids are not very soluble in electrolyte solutions. To reduce the mass transfer resistance inherent in such systems, several design approaches are generally taken, such as the use of two-phase flow, homogeneous catalysis, and porous electrodes.

Dispersions of a reactant phase in electrolyte solutions have been introduced into electrochemical cells to provide the greatly enhanced mass transfer rates needed for practical cell operation. Several such two-phase systems have been studied on a pilot scale, and include oxygen electrodes for the production of hydrogen peroxide (Oloman and Watkinson, 1976, 1979), packed bed electrodes for wastewater treatment (Ehdaie et al., 1982), and electroorganic processes (Ellis and Jansson, 1983). Substantial federal investment in the research and development of oxygen electrodes for chlorine production and fuel cell applications is also indicative of the potential economic importance of two-phase electrochemical systems. Engineering development of such two-phase flow cells is critically dependent on improved understanding of mass transport processes in these cells.

It is well known that the rates of reactant absorption from a dispersed phase and consumption at the solid surfaces are increased by the elevated fluid velocities and the turbulent nature of two-phase flow. In addition, recent work has shown that penetration of the solid-liquid mass transfer boundary layers, at the electrode surface, by reactive bubbles or droplets dispersed in the electrolyte, allows absorbing reactants to bypass much of the resistance to mass transfer that would otherwise be experienced by reactants in the bulk aqueous phase. Figure 1 depicts the particle boundary layers δ_1, bubble boundary layers δ_2, and penetrated regions that are bounded by bubble and solid surfaces δ_3. The relative importance of each region is defined by its specific surface area, a, and characteristic thickness $\delta = D/k_i$.

Interaction between solid and dispersed-phase boundary

The present address of K. M. Takahashi is AT&T Bell Laboratories, Murray Hill, NJ 07974.

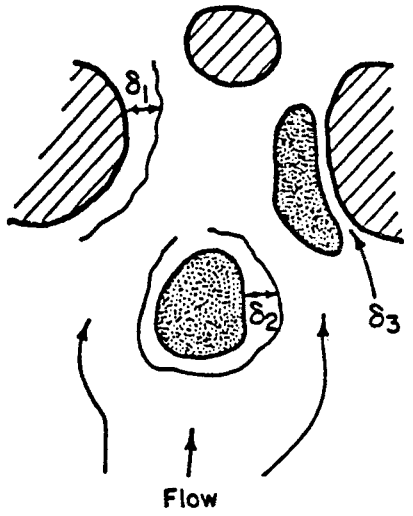

Figure 1. Boundary layer regions, of thickness δ.
1. Particle boundary layer
2. Bubble boundary layer
3. Penetration region

layers was first reported by Lu and Alkire (1984) for the case of aqueous/dispersed-organic flow in a parallel plate cell. They found that in the presence of a flowing aqueous solution at equilibrium with dispersed organic droplets containing concentrated reactant, electrode currents were much higher than those measured in the presence of an aqueous solution of equivalent composition and reactant-free droplets.

Economou and Alkire (1985) showed experimentally that addition of as little as a 10% volume fraction of reactive bubbles to saturated solution flowing in a parallel plate cell increased the overall mass transfer rate by 700% while only increasing pumping power by 22% and IR losses by 15%. Half of the mass transfer increase was shown to arise from boundary layer penetration. Takahashi and Alkire (1985) demonstrated that addition of reactive bubbles to electrolyte flow through a packed bed electrode increased the rate of mass transfer to the electrode surfaces by as much as 350%; most of the enhancement was attributed to boundary layer penetration. These studies provide unambiguous experimental evidence that boundary layer penetration by a dispersed second phase is a dominant mass transfer process in these representative two-phase flow cells.

Mass transport in penetration regions is particularly important when a dissolved redox catalyst is present during electrolysis. Such homogeneous catalysts have the capability of decreasing both charge transfer and mass transfer limitations. As a result, they have received considerable attention for the promotion of the technologically important oxygen reduction and electroorganic synthesis reactions (Simonet, 1983), for which such limitations are particularly severe. Improved understanding of reaction-enhanced mass transfer in penetration regions is thus critically important to the design of reaction-mediated two-phase systems.

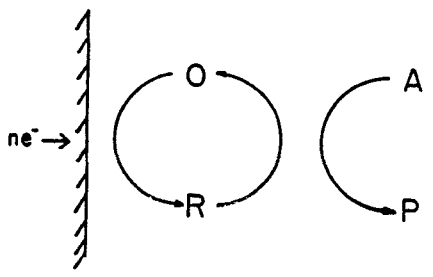

Figure 2. Indirect electrochemical reduction of reactant *A* by a redox couple.

The mechanism of redox catalysis is shown in Figure 2. The desired electrode reaction (reduction in this paper)

$$A + ne^- \rightarrow \nu_p P \tag{1}$$

may be kinetically sluggish, and may be mass transfer limited owing to the low solubility of A in electrolyte solutions. In a redox-mediated system, the electrode reaction is replaced with that of a soluble redox couple

$$\nu_o O + ne^- \rightarrow \nu_R R \tag{2}$$

The reduced catalyst R reacts in solution with dissolved reactant to produce the desired product and to regenerate the catalyst.

$$\nu_R R + A \rightarrow \nu_p P + \nu_o O \tag{3}$$

The net result of reactions 2 and 3 is the desired overall reaction 1. The slow electrode reaction, 1, is replaced by a facile electrode reaction, 2. Mass transfer is enhanced by the substitution of a dilute reactant A by a concentrated catalyst O, and by homogeneous regeneration of catalyst, reaction 3, within the mass transfer boundary layer.

The rate of electrochemical reaction, Eq. 2, depends on the local electrode potential and the concentrations of electroactive species O and R at the electrode surface. This rate must be matched by stoichiometric fluxes of reactants and products to and from the electrode surface. In penetration regions, the effect of mass transfer can thus be incorporated into a model of potential-dependent electrode reaction rate in the form of a relationship between reactant flux (current density) and solution composition at the electrode and bubble surfaces that bound the region. In this study, a diffusion layer model is used to derive equations relating solution composition and reaction-enhanced species fluxes at both bubble and electrode surfaces in penetration regions. In addition, a method to obtain model parameters k_p and a_p (penetration mass transfer coefficient and specific surface area, respectively) from experimentally measurable quantities is described.

Theory

Reaction-enhanced mass transfer in penetration regions

A steady-state thin film model can be used to predict reaction enhanced mass transfer rates in penetration regions. Reactant concentrations in the penetration regions are described as functions of distance x from bubble surfaces by the equations

$$D_A \frac{d^2 C_A}{dx^2} = k_r C_A^n C_R^m \tag{4}$$

$$D_R \frac{d^2 C_R}{dx^2} = \nu_r k_r C_A^n C_R^m \tag{5}$$

and boundary conditions

$$\text{at } x = 0, \quad C_A = C_A^{\text{sat}} \tag{6}$$

$$\frac{dC_R}{dx} = 0 \tag{7}$$

$$\text{at } x = \delta_p, \quad C_R = C_R^s \tag{8}$$

$$\frac{dC_A}{dx} = 0 \tag{9}$$

At the bubble surface ($x = 0$), the reactant is at equilibrium with the gas phase, while catalyst is unable to enter the gas phase. At the particle surface ($x = \delta_p = D_R/k_p$), the reduced catalyst has some concentration C_R^s, which can be specified as a boundary condition for the purpose of the mass transfer calculations. Depending on the rate of surface reaction, C_R^s lies between 0 (slow surface reaction) and the total catalyst concentration C_{cat} (mass transfer control). The rate of direct reduction of the reactant A at the electrode surface is considered to be negligible.

The chemical reaction, Eq. 3, will go essentially to completion as long as the equilibrium potential of the catalyst couple is more than about 100 mV cathodic with respect to the reactant/product couple. As a result, the concentration of P will not affect absorption rates. The concentration of O can then be related to that of R at every position in a boundary layer region by

$$C_o = C_o^b - \frac{\nu_O D_R}{\nu_R D_O}(C_R - C_R^b) \tag{10}$$

where the superscript b refers to the bulk solution outside the penetration region.

With the use of scaling arguments:

$$x^* = \frac{x}{\delta_p} \tag{11}$$

$$A^* = \frac{C_A}{C_A^{\text{sat}}} \tag{12}$$

$$R^* = \frac{C_R}{C_{\text{cat}}} \tag{13}$$

where

$$C_{\text{cat}} = C_R^b + \frac{\nu_R C_O^b}{\nu_O} \tag{14}$$

Equations 4–9 become

$$\frac{d^2A^*}{dx^{*2}} = C_c\phi_p A^{*n} R^{*m} \tag{15}$$

$$\frac{d^2R^*}{dx^{*2}} = \phi_p A^{*n} R^{*m} \tag{16}$$

$$\text{at } x^* = 0, \quad A^* = 1 \tag{17}$$

$$\frac{dR^*}{dx^*} = 0 \tag{18}$$

$$\text{at } x^* = 1, \quad \frac{dA^*}{dx^*} = 0 \tag{19}$$

$$R^* = R_s^* \tag{20}$$

where

$$\phi_p = \frac{\nu_R k_r (C_A^{\text{sat}})^n (C_{\text{cat}})^{m-1} D_R}{k_p^2} \tag{21}$$

and

$$C_c = \frac{C_{\text{cat}} D_R}{\nu_R A^{\text{sat}} D_A} \tag{22}$$

The parameter ϕ_p represents the relative rate of chemical reaction to diffusion in the penetration region, and is a form of the Damköhler number. The parameter C_c is a ratio of catalyst-to-reactant concentrations, and characterizes the ability of the catalyst to enhance mass transfer rates in the penetration region compared to those of an electroactive reactant without catalyst.

To find a relationship between particle current density and surface composition, rather than detailed concentration profiles within the penetration region, the following approach was taken.

In the neighborhood of the bubble surface ($x^* = 0$), the reduced catalyst concentration has some unknown value R_B, which is nearly constant in x according to Eq. 18. The concentration of A in this neighborhood is therefore described by

$$\frac{d^2A^*}{dx^{*2}} = (C_c\phi_p R_B^{*m}) A^{*n} \tag{23}$$

in which the number in parentheses is nearly constant, with the result that Eq. 23 can now be solved. Van Krevelen and Hoftijzer (1948) and Hikita and Asai (1964) applied a similar approximation to the problem of chemical absorption from bubbles, and found that the predicted fluxes compared extremely well to experimental results and exact numerical calculations.

Based on the assumptions of fast reaction ($\phi_p > 1$) and concentrated catalyst ($R_s^* C_c > 1$), integration of Eqs. 15 and 16 yields:

$$R_B^* = \frac{1}{C_c}(R_s^* C_c - \Xi + 1) \tag{24}$$

and therefore from Eq. 23,

$$\Xi^{2/m} + K\Xi - K(R_s^* C_c + 1) = 0 \tag{25}$$

where

$$\Xi = -\left.\frac{dA^*}{dx^*}\right|_0 = C_c \left.\frac{dR^*}{dx^*}\right|_1 \tag{26}$$

and

$$K = \frac{1}{C_c}\left(\frac{2\phi_p}{n+1} C_c\right)^{1/m} \tag{27}$$

Two important analytical solutions exist. When $m = 1$,

$$\Xi = \left[\frac{\phi_p}{n+1}\left(\frac{\phi_p}{n+1} + 2R_s^* C_c + 2\right)\right]^{1/2} - \frac{\phi_p}{n+1} \tag{28}$$

and when $m = 2$,

$$\Xi = \frac{\left(\frac{2\phi_p}{n+1}\right)^{1/2}(1 + R_s^* C_c)}{C_c^{1/2} + \left(\frac{2\phi_p}{n+1}\right)^{1/2}} \tag{29}$$

By requiring that a catalyst have a reasonably high solubility and reactivity, it is thus possible to take advantage of van Krevelen's approximation and the boundary condition type to derive an approximate relationship between current density and surface concentration of catalyst.

Exact numerical solutions of Eqs. 15–20 were also obtained by using a variable step size finite difference program, details of which can be found elsewhere (Takahashi, 1986). Comparison between the "exact" and approximate solutions is made below.

Determination of penetration area and film thickness

To apply the mass transfer model described above to the prediction of surface fluxes, it is necessary to know the mass transfer coefficient k_p and the specific surface area a_p, not just the experimentally measurable product $k_p a_p$. The independent measurement of penetration parameters k_p and a_p is a difficult task, owing to the number of other mass transfer processes that simultaneously take place. However, there exists a geometric relationship between the depth and area of boundary layer penetration by bubbles, which makes k_p and a_p separable. That relationship was approximated by the following model.

Particle boundary layers are modeled as thin films having a mean thickness $\delta_L = D/k_L$ that is determined by measurement of k_L. Figure 3 illustrates the situation when a spherical bubble penetrates the particle boundary layers to an average solid angle of θ. The projected area of penetration of this bubble is

$$A_\theta = \pi R^2 \sin^2\theta \tag{30}$$

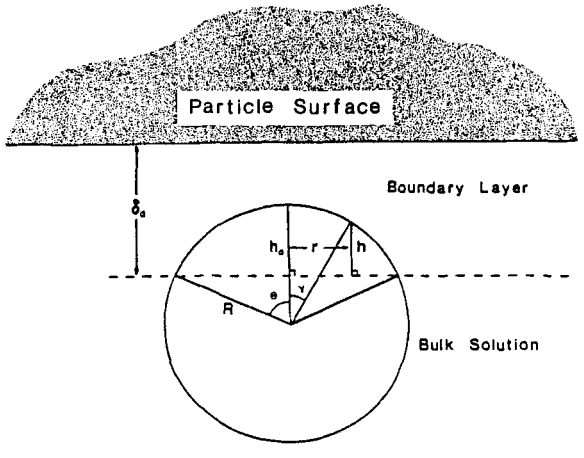

Figure 3. Penetration region formed between spherical bubble and solid electrode surface.

and the penetration depth is

$$h = R(\cos\gamma - \cos\Theta) \tag{31}$$

The average penetration depth $\bar{h}$ is defined by

$$\bar{h} = \frac{\int h dA}{A} = \frac{R}{\sin^2\theta}\left(\frac{\cos^3\theta}{3} + \frac{2}{3} - \cos\theta\right) \tag{32}$$

Equations 30 and 32 give the desired relationship between penetration area and depth for a single bubble. To find the total area, the surface density of penetrating bubbles must be estimated.

β_G is the gas holdup, or gas fraction within the packing voids. The average bubble diameter is:

$$d = \frac{6\epsilon\beta_G}{a_G} \tag{33}$$

based on the assumption that β_G is the same near the particles as it is in the bulk solution. As will be shown below, this assumption is not critical. The number density of bubbles is:

$$N = \frac{\beta_G}{V_b} = \frac{6\beta_G}{\pi d^3} \tag{34}$$

A typical bubble near the solid surface occupies a cube having the volume

$$V_{\text{cube}} = \frac{1}{N} + d^3\left(1 - \frac{\pi}{6}\right) = d^3\left[1 + \frac{\pi}{6}\left(\frac{1}{\beta_G} - 1\right)\right] \tag{35}$$

with an accessible volume of $1/N$. The length of the box edge is

$$L = d\left[1 + \frac{\pi}{6}\left(\frac{1}{\beta_G} - 1\right)\right]^{1/3} \tag{36}$$

The electrode surface is covered with such boxes. The probability of a bubble in a surface box penetrating the boundary layer is given by:

$$P_{\text{pen}} = \frac{\delta_L}{L - d} \tag{37}$$

when $L - d > \delta_L = D/k_L$. If $L - d < \delta_L$, then the probability of penetration is unity, so the specific area for penetrating bubbles can now be defined:

$$a_p = a_s \frac{\pi R^2 \sin^2\theta}{(1/N)^{2/3}} \min\left(1, \frac{\delta_L}{L - d}\right) \tag{38}$$

and the mass transfer coefficient is:

$$k_p = \frac{D}{\delta_L - \bar{h}} \tag{39}$$

The only unknown independent variable in Eqs. 32 to 39 is θ, the penetration angle. The angle can be determined by combining these equations and equating the product $k_p a_p$ to measured val-

ues. The system of Eqs. 32 to 39 was solved numerically, using a program described by Takahashi (1986). As described below, the penetration angle θ was determined for a wide range of flow conditions, and was used to calculate a_p and k_p, given required values of other mass transfer parameters and physical properties.

Results and Discussion

Chemical reaction in penetration regions

The solution of Eqs. 15 through 20 was obtained both by the use of a finite difference calculation and by the use of an approximate solution, Eq. 25, for (m, n)-order irreversible homogeneous reaction. The results of the calculations shown in Figure 4 for (2, 1)-order kinetics indicate a good match between the "exact" and approximate theories. The approximate solution is based on the assumptions of fast reaction ($\phi_p \gg 1$) and concentrated catalyst ($R_s^* C_c \gg 1$). In general, the surface composition depends on kinetic processes that occur at the solid surface. For the purpose of comparison with numerical results, R_s^* is set at unity, which corresponds to the condition of mass transfer control. The approximate solution agrees with the numerical solution to within 2.0% when C_c and ϕ_p are greater than 3.

Figure 5 shows the approximate solution, Eq. 29, on an expanded scale. Two important limiting cases stand out. At high values of ϕ_p, the dimensionless flux (current density) approaches a limiting value that corresponds to the case of instantaneous kinetics. Under such circumstances, reaction occurs at a plane between the bubble and particle surfaces, and the dimensionless current density of Eq. 29 reduces to

$$\Xi = 1 + R_s^* C_c \tag{40}$$

The condition of instantaneous reaction is met for (2, n)-order kinetics when

$$\sqrt{\frac{2\phi_p}{C_c(n+1)}} \gg 1 \tag{41}$$

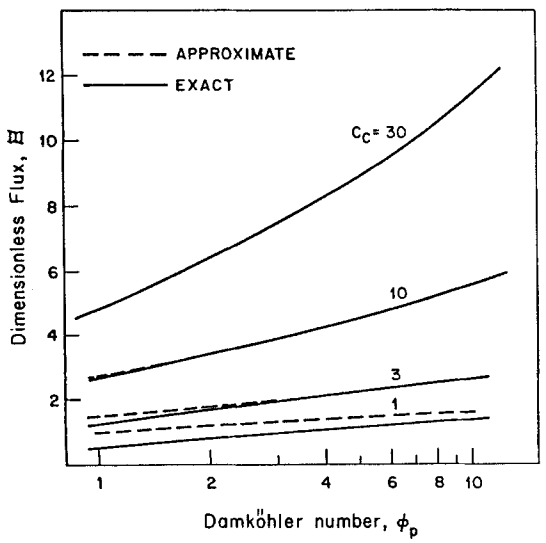

Figure 4. Dimensionless flux in penetration regions, (2, 1)-order kinetics.

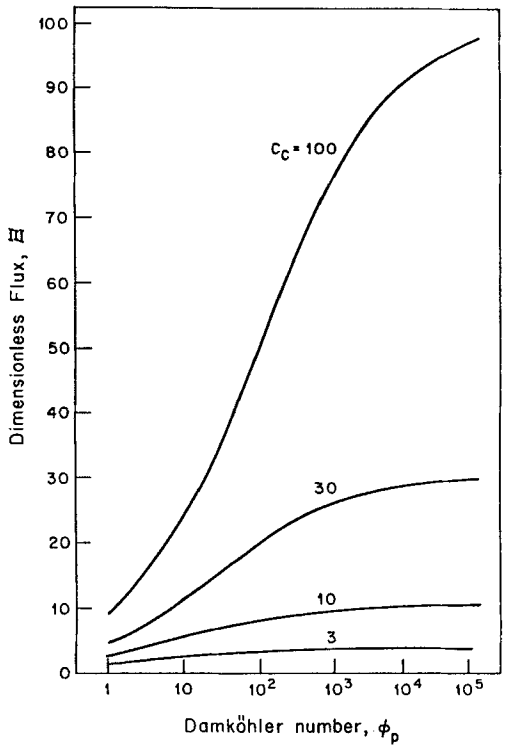

Figure 5. Approximate solution, (2, 1)-order kinetics.

The other limit occurs when the reaction rate is low. Although the approximate solution does not apply when $\phi_p < 1$, it correctly predicts that as ϕ_p approaches zero, so does the current density. The fact that the electrode reactant O can only be made available by homogeneous oxidation of R by A is in contrast to the other boundary layer regions, which can exchange mass with the bulk solution even in the absence of homogeneous reaction.

In reality, the reactant A can often react directly at the electrode surface, albeit at kinetically inhibited rates, if it is not first consumed by homogeneous reaction. Even at extreme potentials, however, this current will be low, on the order of $1/C_c$ times that of the redox-active penetration regions. It is fair to say, then, that the penetration regions are essentially inactive when $\phi_p \ll 1$.

The approximate solution, Eq. 28, for (1, 1)-order kinetics, Figures 6 and 7, is qualitatively the same as that for (2, 1)-order kinetics. The asymptotic limit is also given by Eq. 40, and is reached when the condition

$$\frac{\phi_p}{2(n+1)(C_c+1)} \gg 1 \tag{42}$$

is met. Equation 28 agrees with 0.9% with the exact numerical solution when ϕ_p, $R_s^* C_c > 3$.

Determining the relationship between current density and surface concentrations of reduced (Eq. 25) and oxidized (Eq. 10) catalyst provides a means for treating the coupling of transport processes in penetration regions with kinetic processes at the electrode surface. The steady-state thin film model provides a simple but complete description of reaction-enhanced mass transfer in these regions. The film model may not describe the physical process of boundary layer penetration as realistically as surface renewal models. However, it is likely that, as in the case

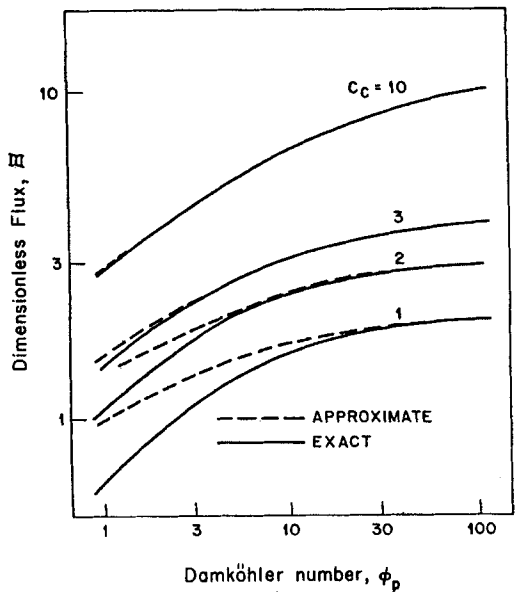

Figure 6. Dimensionless flux in penetration regions, (1,1)-order kinetics.

of reaction-enhanced mass transfer from bubbles (Danckwerts, 1970), both the film models and renewal models provide excellent predictions of reaction-enhanced mass transfer rates in bubble-penetrated boundary layers.

Thickness and area of penetrated regions

In order to calculate the Damköhler number, it is necessary to know the penetration film thickness, or equivalently, the mass transfer coefficient. The film thickness cannot in general be measured, so a spherical-bubble model is used to estimate it. While the spherical-bubble model cannot be considered to be a precise representation of the geometric relationship between k_p and a_p, it will be shown that numerical values fall within the expected ranges, even for gas-continuous flow in which the concept of a bubble is inappropriate. The model provides useful estimates of transport parameters that have never been measured for any but the simplest of two-phase flows.

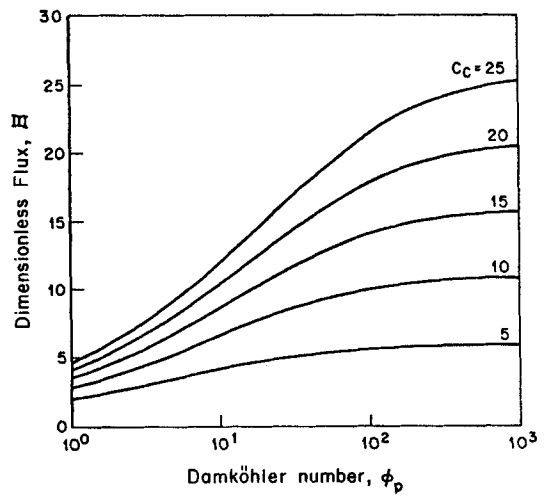

Figure 7. Approximate solution, (1,1)-order kinetics.

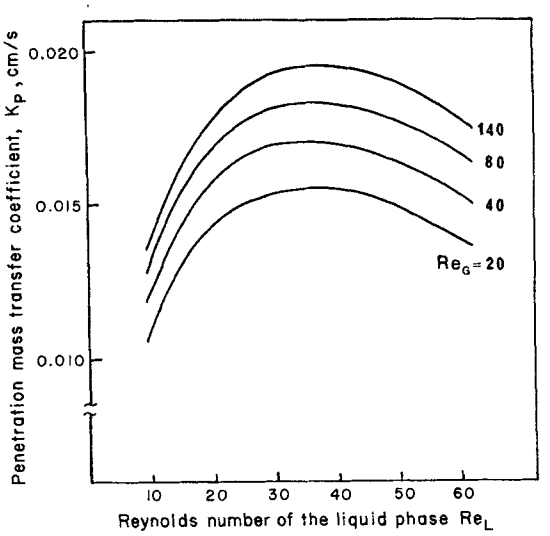

Figure 8. Mass transfer coefficients.
Calculated from data of Takahashi and Alkire (1985, 1988)

Use of the model requires a knowledge of the parameters $k_p a_p$, a_s, a_G, β_G, ϵ, and k_L. The mass transfer parameters have been measured by Takahashi and Alkire (1985) and Takahashi (1986) in a packed bed consisting of 1.2 mm glassy carbon particles for a wide range of gas/liquid flow rates. Values of k_p and a_p calculated for this experimental system are shown in Figures 8 and 9. All the properties and parameters required for the calculation of k_p and a_p were known except for the gas holdup, β_G. As is evident in the formulation of the penetration model, the value of β_G chosen for the calculation has a strong effect on the estimated values of bubble size and number density of penetrating bubbles. By varying the input value of β_G in the range of 0.2 to 1, these effects on the output variables were indeed observed. Fortuitously, however, the value of β_G had almost no effect on

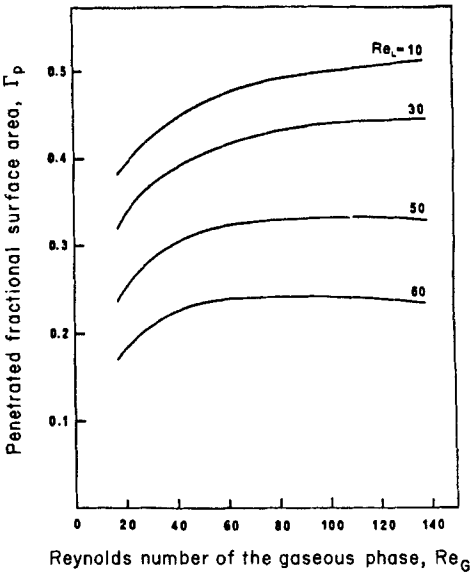

Figure 9. Fractional coverage of solid surface by penetrating bubbles.
Calculated from data of Takahashi and Alkire (1985, 1988)

the resultant values of k_p and a_p, causing a variation of less than 2%. For the results shown in Figures 8 and 9, a value of $\beta_G = 0.5$ was used.

The average penetration angle Θ ranges from 26° for very fine bubble dispersions ($Re_L = 60$, $\bar{d} < 10$ μm) to 70° near the gas-continuous limit ($Re_L \approx 15$). The corresponding mass transfer coefficients are comparable to, but greater than, liquid-solid coefficients k_L under the same flow conditions. As shown in Figure 8, k_p increases with both Re_L and Re_G when $Re_L < 35$. However, plots of k_p vs. Re_L go through maxima when $Re_L \approx 35$, which corresponds to an average bubble size on the order of 50 μm (Takahashi and Alkire, 1988). As Re_L increases beyond 35, liquid inertia may force bubbles away from particle impingement points, decreasing boundary layer penetration. In this velocity region, Reynolds numbers based on mean bubble diameter and liquid velocity are on the order of unity. Penetration by the larger than average bubbles would be particularly inhibited by inertial effects. Buoyant rise velocities are small (less than 5% of liquid velocities) when $Re_L > 35$, and thus do not contribute to penetration by enhanced impingement.

Figure 9 shows that penetrated area decreases with Re_L, and is relatively insensitive to gas velocity for $Re_G > 60$. Predicted plateau coverage ranges from 0.22 of the particle area for small-bubble/high-Re_L flows, to 0.5 for gas-continuous flow ($Re_L = 10$). Weak penetration at high liquid velocities again suggests an inertial effect. High coverage at low Re_L indicates the presence of bubbles comparable in size to packing voids. These bubbles must conform to packing particle surfaces, resulting in extensive thin-film penetration regions.

Conclusions

When a homogeneous catalyst is present in the region of impingement of reactant-bearing bubbles on solid surfaces, the concentration driving force is not limited by the solubility of the gaseous reactant, but by the potentially high concentration of the catalyst couple. At low liquid flow rates when penetration areas are extensive, transport and reaction in these regions plays a key role in determining the ability of a redox catalyst to promote in-cell absorption of gaseous reactants.

Reaction-enhanced transport in penetration regions was described by a diffusion layer model. An approximate solution of the model equations was obtained for (m, n)-order irreversible homogeneous kinetics. The approximate solution was in the form of an implicit algebraic relationship between surface concentration and flux of catalyst. Surface flux was obtained as an explicit function of surface concentration for the cases of $(1, n)$- and $(2, n)$-order kinetics. These explicit functions were in a form useful for the treatment of mass transfer coupled with kinetic processes at solid surfaces. The approximate solutions agreed with exact numerical solutions of the model equations in the regime of fast homogeneous reaction and concentrated catalyst (ϕ_p, $R_s^* C_c > 3$).

Penetration regions are bounded by bubble and solid surfaces, and do not interact with the bulk solution. Surface reaction of the catalyst cannot take place at steady state, therefore, unless the catalyst is regenerated by homogeneous reaction. When the Damköhler number is less than unity, homogeneous reaction is ineffective at replenishing the catalyst, and penetration regions are essentially inactive.

At the other extreme, high values of ϕ_p produce limiting values of catalytic currents. The value of ϕ_p required to produce the condition of instantaneous kinetics depends on catalyst concentration and reaction rate order. For $(1, n)$- and $(2, n)$-order kinetics, the parameter spaces corresponding to instantaneous kinetics were defined.

A small-bubble penetration model was derived to estimate penetration film thickness and specific surface area from mass transfer parameters that can be measured directly. Penetration parameters were calculated for gas-liquid flow in a packed bed in which the other mass transfer phenomena have been experimentally characterized. Mass transfer coefficients were found to increase with gas Reynolds number, but had maxima in liquid Reynolds number when $Re_L \approx 35$. With increasing Re_L values, liquid inertia prevented bubbles from impinging on packing particles, and k_p decreased. Penetration area was found to decrease monotonically with Re_L, and was relatively insensitive to Re_G.

Acknowledgment

Financial support for this study was provided by the American Chemical Society, ACS Grant No. 16437-7, 3C. Fellowship support was provided by the General Electric Corporation, Exxon Corporation, and Eastman Kodak Company.

Notation

a = specific surface area, m^{-1}
A = reactant species
C = concentration, mol/m^3
C_c = dimensionless catalyst concentration, $C_{cat} D_R / \nu_R A^{sat} D_A$
d = bubble diameter, m
D = diffusivity, m^2/s
h = penetration depth, m
k = mass transfer coefficient, m/s
k_r = homogeneous rate constant, $kmol/m^3 \cdot s$
L = length of box edge, m
N = number density of bubbles, m^{-3}
O = oxidized catalyst species
P = product species
R = reduced catalyst
Re = particle Reynolds number
V = volume, m^3
x = distance from bubble surface, m

Greek letters

β_G = fractional gas holdup
ϵ = void fraction of the packed bed
γ = angle, rad
Γ = fractional surface area, a_p/a_s
δ = boundary layer thickness, m
θ = penetration angle, rad
ν = stoichiometric number
Ξ = dimensionless flux
ϕ = Damköhler number

Superscripts

b = bulk solution
m = rate order in catalyst species R
n = rate order in reactant A; number of electrons, equiv/mol
s = surface
sat = saturated
* = dimensionless parameter

Subscripts

A = reactant
B = bubble surface
cat = catalyst
G = gas
L = liquid
O = oxidized catalyst

p = penetrated boundary layer
P = reaction product
R = reduced catalyst

Literature Cited

Danckwerts, P. V., *Gas-Liquid Reactions,* McGraw-Hill, New York (1970).

Economou, D. J., and R. C. Alkire, "Two-Phase Mass Transfer in Channel Electrolyzers with Gas-Liquid Flow," *J. Electrochem. Soc.,* **132,** 601 (1985).

Ehdaie, S., M. Fleischmann, and R. E. W. Jansson, "Application of the Trickle Tower to Problems of Pollution Control. I: The Scavenging of Metal Ions," *J. Appl. Electrochem.,* **12,** 59 (1982).

Ellis, K. G., and R. E. W. Jansson, "The Indirect Electrochemical Epoxidation of Butenes and Ethylene in a Bipolar Trickle Tower," *J. Appl. Electrochem.,* **13,** 657 (1983).

Hikita, H., and S. Asai, "Gas Absorption with (m, n)th-Order Irreversible Chemical Reactions," *Int. Chem. Eng.,* **4,** 332 (1964).

Lu, P. Y., and R. C. Alkire, "Mass Transfer in Parallel Plate Electrolyzers with Two-Phase Liquid-Liquid Flow," *J. Electrochem. Soc.,* **131,** 1059 (1984).

Oloman, C., and A. P. Watkinson, "Electrolytic Production of Alkaline Peroxide Solutions," U.S. Pat. 3,969,201 (July, 1976).

———, "Hydrogen Peroxided Production in Trickle Bed Electrochemical Reactors," *J. Appl. Electrochem.,* **9,** 117 (1979).

Simonet, J., "Electrogenerated Reagents," *Organic Electrochemistry,* 2d ed., M. M. Baizer and H. Lund, eds. Dekker, New York (1983).

Takahashi, K. M., "Homogeneous Catalysis in Flow-by Porous Electrodes Containing Gas-Liquid Flow," Ph.D. Thesis, Univ. Illinois, Urbana (1986).

Takahashi, K. M., and R. C. Alkire, "Mass Transfer in Gas-Sparged Porous Electrodes," *Chem. Eng. Commun.,* **38,** 209 (1985).

———, "Mass Transfer from Dispersed Bubbles to Electrolyte Solution in Packed Beds," *AIChE J.,* **34**(9) (Sept., 1988).

van Krevelen, D. W., and D. W. Hoftijzer, "Kinetics of Gas-Liquid Reactions. I: General Theory," *Rec. Trav. Chim.,* **67,** 563 (1948).

Manuscript received Mar. 5, 1987, and revision received June 7, 1988.